Intranasal Diamorphine Population Pharmacokinetics and Dose Regimen Optimization in Pediatric Breakthrough Pain

by

Lianjin Cai

Bachelor of Science, China Pharmaceutical University, 2021

Bachelor of Science, University of Strathclyde, 2021

Submitted to the Graduate Faculty of the

School of Pharmacy in partial fulfillment

of the requirements for the degree of

Master of Science

University of Pittsburgh

2023

UNIVERSITY OF PITTSBURGH

SCHOOL OF PHARMACY

This thesis was presented

by

Lianjin Cai

It was defended on

April 5, 2023

and approved by

Junmei Wang, Associate Professor, Pharmaceutical Sciences

Raman Venkataramanan, Professor, Pharmaceutical Sciences

Lirong Wang, Assistant Professor, Pharmaceutical Sciences

[Thesis Advisor]: Junmei Wang, Associate Professor, Pharmaceutical Sciences

Intranasal Diamorphine Population Pharmacokinetics and Dose Regimen Optimization in Pediatric Breakthrough Pain

Lianjin Cai, B.S

University of Pittsburgh, 2023

Diamorphine hydrochloride (Pharmaceutical heroin) is licensed in the United Kingdom in Accident and Emergency department for breakthrough pain management. Intranasal diamorphine (IND) might represent an acceptable alternative for the pediatric population offering a less traumatic, effective, and expedient treatment. However, the current weight-based dose regimen of pediatrics IND is historical and empirical, relying on clinical expertise and the developmental Pharmacokinetics (PK) properties are poorly understood in children. This study aimed to **(i).** develop a population PK (pop-PK) model in adults following a single small dose of IND and **(ii).** extrapolate the model to the pediatric population with allometry (size) and maturation function (age), with the goal **(iii).** to devise a pediatric dosing regimen that yields a comparable morphine exposure to adults.

The pop-PK analysis of plasma concentrations of diamorphine, 6-monoacetylmorphine, and morphine was conducted utilizing the software package Monolix (v2021R1). The development PK data was collected from two open-access reports of "snorted heroin" published by the National Institute on Drug Abuse (Baltimore). Using nonlinear mixed-effect modeling, an integrated four-compartment pop-PK model with linear absorption and elimination provided an appropriate fit. The estimated IND relative bioavailability was ~ 52% with an indistinguishable first-order absorption rate constant compared to intramuscularly injected diamorphine. The external evaluations confirmed that the model is useful to extrapolate outside the development

dataset scope incorporating the covariates of weight and age, which attains an acceptable average fold error for morphine C_{max} (0.95) as well as for AUC_{0-t} (0.80). More importantly, the predicted morphine concentration-time profiles were basically in agreement with the observed PK data in children after a single dose of IND (0.1 mg/kg). The model-based simulation showed that children cannot achieve a similar morphine exposure compared to adults using the current dosing regimen. Thus, we proposed a dosing scheme that uses optimal doses for different age groups based on PK examination, which recommended that infants less than 6 months should start with a low dosage of IND (0.085 mg/kg) while others require a higher initial dose (0.12-0.125 mg/kg). This PK-guided dosing equivalence using similar exposure at different ages could become a reasonable starting point for the clinical usage of nasal diamorphine spray, before individualized adjustments with the varying pain experience.

Table of Contents

List of Tables

List of Figures

Preface

I would like to express my sincerest gratitude to my advisor, Dr. Junmei Wang. His invaluable guidance and unwavering support played a crucial role in helping me start and successfully complete my project. Dr. Wang not only shared his expertise and knowledge, but also his work ethic and approach to life, which have highly impacted me.

I am also deeply grateful to my committee members, Dr. Raman Venkataramanan and Dr. Lirong Wang, for their insightful feedback and advice, which greatly contributed to the quality of my thesis.

I extend my heartfelt appreciation to all the members of our lab group and senior graduate students from Dr. Venkat's group and Dr. Wang's group, whose unwavering encouragement and support helped me overcome obstacles during the project.

I would also like to acknowledge the endless support and love of my parents, who have been my pillars of strength throughout my academic journey.

Lastly, I offer my regards and blessings to all of those who supported me in any respect during the completion of my project.

1.0 Introduction

1.1 Diamorphine Medical Usage: Pediatric Breakthrough Pain

Diamorphine hydrochloride (DIAM, pharmaceutical heroin) has been medically used in many Europe countries for refractory heroin dependents who have not responded to the standard maintenance treatment, albeit prohibited in the United States (USA). [1] Interestingly, DIAM is also prescribed in the United Kingdom (UK), as a strong opioid and the prodrug of morphine, for breakthrough pain management in the setting of Accident and Emergency (A&E) as well as palliative care.[2-4] Breakthrough pain is described as severe pain that occurs with episodes of sudden onset despite the regular background opioid treatment given. It raises great challenges because of the few suitable potent, well-tolerated, and fast-acting agents available to manage this pain exacerbation in life-limiting conditions. [2,3] Oral morphine (MOR) is a usual first-line treatment for children, yet it often takes more than 30 min to achieve the target concentration and to produce an analgesic effect. [5] Although injections (intravenous, subcutaneous, and intramuscular) allow faster onset, supervised needle usage inevitably delays pain relief because of the poor acceptability for children and the stress to parents and clinical practitioners. A needle-free, fast-acting pain medicine is needed.

Diamorphine is a semisynthetic diacetylated derivative of morphine, and its many advantageous properties render it a desirable analgesic agent via transmucosal administration (sublingual, intranasal, or buccal). It is considered as a morphine prodrug with approximately twice the potency as morphine salt. [6] The needle-free and parenteral transmucosal delivery results in rapid systemic absorption across richly vascularized mucosa avoiding first-pass metabolism. The

lipophilicity of DIAM enables its quick distribution and passage through the blood-brain barrier once it enters the systemic circulation. Furthermore, the rapid metabolism of DIAM to the active intermediate metabolite, 6-monoactylmorphine (MAM) is responsible for the early analgesia onset (maximum effect within 10 min), and sequentially to morphine, exerting a potent and lasting pharmacological effect (maximum effect within 1 h). [7] [8] The esterase, abundantly distributed in blood and various organs including the brain and liver (**Figure 1**), sequentially produces both metabolites, which bind to the opioid mu receptors with different affinity and potency. **[9]** Morphine is in turn eliminated by Phase II metabolism, glucuronidation, and subsequent excretion in the urine in the form of morphine-3-glucuronide (M3G) and morphine-6-glucuronide (M6G).

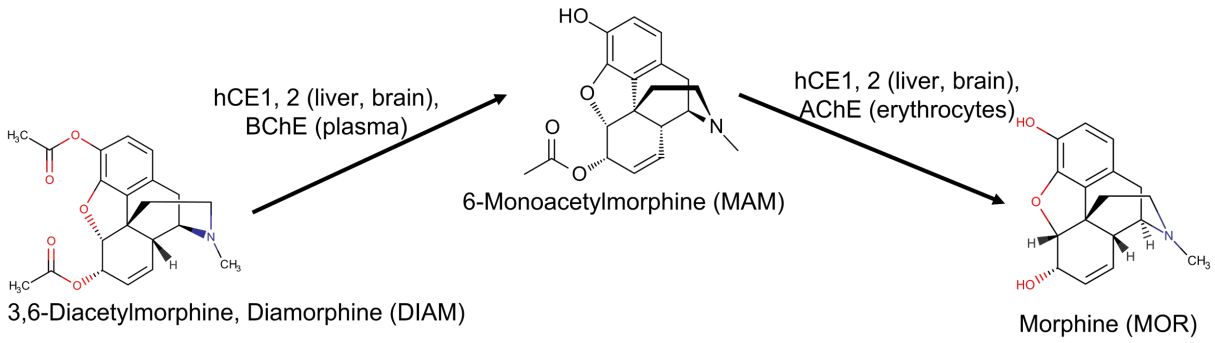

Figure 1. Hydrolytic pathway of heroin in humans executed by various esterases. hCE – human carboxylesterase; BChE – butyrylcholinesterase; AChE – acetylcholinesterase.

1.2 Diamorphine Nasal Spray

Specifically, the "snorted" intranasal diamorphine (IND) has been identified as an acceptable alternative offering less traumatic, effective, and expedient analgesia for the pediatric population.[10] Diamorphine hydrochloride nasal spray (IND product, Ayendi®) has been licensed for moderate and severe pain in children and adolescents 2-15 years of age. Previous research had

demonstrated its satisfactory safety profiles and it is as effective as intramuscular diamorphine (IMD) for acute pain in the A&E department. [11-13] However, there is still a paucity of research evidence and clinical guidelines for IND dosing in children. Pediatric clinical studies are challenging to conduct owing to ethical and logistical constraints. Current dosage selection of pediatrics IND is historical and empirical, which is guided by clinical acumen and previous observational studies, rather than the examination of pharmacokinetics (PK) and pharmacodynamics (PD), two important aspects of a drug

The latest British systematic review paper sought, screened, and summarized 19 clinical studies regarding Diamorphine pharmacokinetics, of which only 1 was conducted in children and 2 in neonates.[14] A few studies quantified PK data of diamorphine and metabolite concentration, while most only reported morphine exposure within a variable duration using the area under the plasma concentration-time curve (AUC). The time course of intranasal diamorphine concentration and sequential effects by its active metabolites in children are poorly depicted, despite its extensive use in acute and palliative care settings. The reported PK parameters of DIAM had also been retrieved including AUC, clearance (CL), maximum concentration (C_{max}), the time to C_{max} (T_{max}), the volume of distribution (V_d), and drug half-life ($t_{1/2}$). However, it remains uncertain for children dosing with IND because of the different routes adopted, the incomplete parameter estimates (PE) like the bioavailability ($F_{\%}$) of IND, the lack of age-and-weight standardization, and the usage of non-compartmental analysis (NCA). The empiric NCA method, originally designed to define individual PK profiles, ignores inter-individual variability and potential covariates influence. The developmental changes in pharmacokinetics (PK) and pharmacodynamics (PD) with age add more variability to influence dosage selection in children. [15]

1.3 Population Pharmacokinetics

Population pharmacokinetics (pop-PK) modeling can incorporate covariate information (e.g., demographics information, pharmacogenomics, and concomitant medication) into complicated mathematical and compartmental analysis to explain sources of the PK variability within a population. Understanding PK variability is crucial to ensure safety and efficacy for a particular patient group. It can inform the selection of rational dosage for a given population and enable precision medicine. Moreover, we also can apply pop-PK to investigate model-based bioequivalence and the exposure-response relationship when combined with PD modeling. PK/PD modeling and simulation (PK/PD-MS) has been applied throughout various stages of drug development [16]. The notable examples of simulation techniques include facilitating dose selection for pediatric patients by leveraging data acquired from adults [17], determining starting doses for first-in-human studies based on preclinical and nonclinical data [18] [19], selecting doses for Phase 2 trials on the basis of Phase 1 results [20], modifying doses for Phase 3 trials based on Phase 2 outcomes [21], and serving as a regulatory tool in the drug approval processes [22].

Furthermore, PKPD-MS has proven validity for dosage optimization and clinical translation of drug disposition and effects in pediatric analgesia and anesthesia, [23-25] utilizing allometric scaling theory and maturation model.[26,27] In the case of diamorphine, concentration-time profiles were simulated by Morse et.al to identify reasonable dosages for different age groups of children. But the parameter values fixed in their models were integrated from multiple pop-PK studies without a data fitting process as well as the inclusion of inter-individual variability, and some key information was assumed based on the NCA findings, such as the F% of IND absorption, which was presumed to be 50%.[23] Till now, there is only one pop-PK model has been reported for diamorphine after intravenous and inhalation administrations in heroin-assisted therapy clinical

trials for opioid use disorder, another medical indication of diamorphine. [28] More importantly, the missing step of body-weight standardization precluded the potential to perform model simulation using allometric scaling algorithms.

1.4 Objectives

Again, PK/PD properties of intranasal diamorphine for breakthrough pain relief need further evaluation, and the dosage for the pediatric population remains disputable due to the limited clinical guidelines. Interestingly, some articles years ago provided open-access PK and PD data in numeric format from adults receiving diamorphine through multiple administration routes. [29-31]

Herein, we used the published plasma concentration data of diamorphine and its metabolites obtained in adults to develop a pop-PK model. Covariates modeling was conducted to assess the influential variability factors. Subsequently, the established adult model was extrapolated to the pediatric population using the allometric scaling function with body weight and the maturation function with postmenstrual age (PMA). External validation was also performed to evaluate this model extrapolation. Finally, the simulation-based methodology was leveraged to evaluate the effectiveness of given clinical equianalgesic doses (0.1 mg/kg) and devise an dosing strategy of intranasal DIAM for children of different age groups to target a comparable morphine exposure.

2.0 Methods

2.1 Data Preparation

A Pubmed search was conducted for articles from 1980 till 2022 August to find clinical pharmacokinetics studies concerning diamorphine and its active metabolites (MAM and MOR). The dosage strategy adopted should be close to the medical usage of diamorphine for the indication of breakthrough pain [8]. Consequently, 4 published PK datasets were prepared for this Pharmacometrics analysis, and the data characteristics are summarized in **Table 1**.

The model development datasets were collected and extracted from two clinical PK studies presented by the National Institute on Drug Abuse (Baltimore) that shared the same dosing regimen, study medication, analysis method, and blood sampling time. Both of these studies analyzed the PK after a single dose of intranasal diamorphine (IND, 6mg and 12mg) in comparison with intramuscular diamorphine (IMD, 6mg) in male heroin users, using a double-blind, double-dummy crossover design with a 1-week washout period between three successive administration treatments. In addition, Girardin et. al. recruited 8 heroin-addict patients to assess intramuscular diamorphine with 3 doses (<200-250 mg) [32], whilst Kidd, et. al. employed 12 children aged from 4-13 years to evaluate a single dose of intranasal diamorphine (0.1 mg/kg) [33]. They are both outside the development data scope and used for external verification.

Table 1. Published clinical PK dataset of diamorphine used in our study.

References	Cone et al. [31]		Skopp et al. [29]		Girardin et al. [32]	Kidd et al.[33]
Num. of Subjects	6	6	2	4	8	12
Application Site	IM	IN	IM	IN	IM	IN
Subject Category	I.	I.	I.	I.	II.	III.
Dosage	6-12 mg	12 mg	6 mg	6-12 mg	<200-250 mg	0.1 mg/kg
Study Medication	Diamorphine hydrochloride					
Bioanalysis Method	GC-MS for plasma DIAM, MAM, and MOR				LC/MS for plasma morphine	RIA for plasma morphine
Research Institute	Addiction Research Center, NIDA/NIH, Baltimore, US				University Hospital, Zürich, Switzerland	University of Edinburgh, Edinburgh, UK
Dataset Usage	Model Development				Model External Evaluation (adult)	Model External Evaluation (children)
Data Format	Numeric individual concentration-time profiles				Graphic mean concentration-time profiles & numeric PK parameters	

Subject categories include I. regular heroin users following 3 days of abstinence; II. opioid-dependents in heroin-assisted treatment; III. children in acute severe pain treatment. Bioanalysis methods include radioimmunoassay (RIA), gas chromatography/mass spectrometry (GC/MS), and liquid chromatography–mass spectrometry (LC/MS). NIDH/NIH, National Institute on Drug Abuse (NIDA), and National Institutes of Health (NIH).

The PK data used in this study includes the plasma concentration for diamorphine, 6-monoacetylmorphine, and morphine. During data preparation, the plasma concentration unit was converted from ng/mL to nM (nmol/L) for the parent-metabolite PK model to take into account different molecular weights (369.4, 327.4, and 285.34 g/mol, respectively), due to the sequential deacetylation of two ester bonds (molar ratio of 1.29).

2.2 Software

In this study, we used MonolixSuite version 2021R2 (Lixoft, Antony, France) to develop the pop-PK model of diamorphine administered via intramuscular (IM) and intranasal (IN) routes. Monolix (v2021 R2) is an innovative and user-friendly platform to conduct non-linear mixed effect

(NLME) analysis, which incorporates the efficient estimation algorithm of stochastic approximation expectation-maximization (SAEM), various diagnostic tools, and automatic model-building techniques. [34] The final Pop-PK model was exported to Simulx (v2021R1) to simulate morphine concentration-time profiles with three goals: **(a).** to perform external verifications, **(b).** to evaluate current weight-based dosage regimens of IND on varying age groups, **(c).** to devise an optimal pediatric dosage.

2.3 Pharmacokinetics Analysis

2.3.1 Structure Model

Structural models were designed using a user-defined ordinary differential equation (ODE) written in Mlxtran language (codes provided in Appendix A). The seed was set as 12345 for each NLME run. Since the initial estimates (IE) choosing is important and can accelerate the estimation convergence process [35], we combined literature information of the previous pop-PK model and NCA method via "AutoInit" techniques offered by Monolix [34] to establish IE values of fixed effects. Specifically, the reported estimates of central volumes for DIAM and MOR were input as prior information using Bayesian estimation, while other inaccessible parameters were estimated using Maximum likelihood estimation initialized with NCA calculated values. (**Table S1,** Appendix B)

Due to the sparse sampling for diamorphine and 6-MAM, all PK data of three compounds were used together to develop the sequential pop-PK model directly using a simultaneous approach. Since diamorphine and its intermediate metabolites (MAM) are negligible to detect in

urine [36], we did not take into account renal elimination believing they are fully converted into morphine, which is consistent with the model assumption proposed by Rook. et, al. [28] All metabolic conversion is unidirectional in our model following the first-order kinetics parameterized with two metabolic transfer constant rates (K_{12}, K_{23}), as shown in **Figure 2**.

To begin with, we separately modeled IMD data as the reference group (bioavailability, $F_{\%}$ is regarded as 100% in this study) disposition. In this explorative structure modeling process, the standard one- and two-compartment models combined with the first-order absorption model were tested to determine the best structural model for drug disposition. Due to the non-unidentifiability of the metabolite compartments, a common choice in previous studies is to set all central volumes for metabolites equal to the volume of distribution for parent drugs, such as ketamine [37,38]. However, this might cause biased estimation for metabolite clearances and peripheral compartment volumes. Since morphine is currently available for human use, we also tested the introduction of the morphine central volumes of morphine in the model.

The final structural model of the IMD group was then applied to the whole dataset and initialized all estimates for fixed effects (population parameters) using the Bayesian approach. Following the inclusion of IND data, several models were assessed to describe the intranasal absorption kinetics, such as simple zero- and first-order kinetics with/without lag time and complicated transit models. The model-guided bioavailability of "snorted" diamorphine (IND) compared to the reference IMD group was thus obtained (bioequivalence). Specifically, it was initialized with a reported 50% as prior information using Bayesian estimation. At this stage, the metabolic transfer, distribution, and elimination of DIAM were expected to be similar, once absorbed, regardless of the varying administration routes. Therefore, the PK disposition parameters were estimated simultaneously by pooling IMD and IND plasma concentration data

together, disregarding the differences in absorption and bioavailability, to take maximum advantage of the existing data.

2.3.2 Statistical Model

Once the structural model was finalized, the statistical modeling was subsequently performed to investigate individual model parameter distributions with their covariates as well as correlations and optimize the error model for observed concentration. For random effects, all parameters were modeled with log-normal distribution to control all individual values to stay positive, except for IND bioavailability ($F_{\%}$), which was modeled using logit-normal distribution to control the value within the range of 0-1. The SAEM estimation was parameterized with 2000 maximum iterations and the default large initial value of population random effect (OMEGA = 1) was applied for all parameters. The estimation precision is determined by Fisher Information Matrix calculated via the Stochastic approximation to obtain more reliable estimated standard errors as well as relative standard errors (%RSE).

The available patient demographics information constitutes two continuous covariates (COVs): body weight (WT) and age. The dosage amount and route of administration, as two categorical covariates (CATs), were investigated for their potential impacts on diamorphine absorption and disposition (**Table 2**). Of note, to achieve the final objective of model extrapolation from adults to children, population parameters for this sequential pop-PK model for diamorphine, 6-monoacetylmorphine, and morphine developed in adults were scaled using the allometric function (body weight) and maturation function (age).

In Equation 1, the influence of body weight on all PK parameters was fixed via empirical allometric scaling function, standardized to 70 kg, with the intercompartmental clearances (CL)

scaled to the exponent of 0.75, intercompartment rate constant (K*)* to -0.25 and volumes (V) to 1. [26]

$$CL_i = CL_{pop}\left(\frac{WT}{70}\right)^{0.75} e^{\eta_k}$$

$$K_i = K_{pop}\left(\frac{WT}{70}\right)^{-0.25} e^{\eta_k}$$

$$V_i = V_{pop}\left(\frac{WT}{70}\right)^{1} e^{\eta_V}$$

(Eq. 1)

The morphine clearance from central compartment was combined with a sigmoid maturation model which was developed to predict morphine dose. [39] The postmenstrual age (PMA) with a unit of weeks was introduced to describe the growth changes in central clearance. In Equation 2, The TM_{50} denotes half-life for maturation of clearance and $Hill_{CL}$ denotes steepness of clearance maturation.

$$PMA = 40 + AGE \times 52$$

$$Hill_{CL} = 3.58;\ TM_{50} = 58.1$$

$$CLi = CL_{pop}\left(\frac{WT}{70}\right)^{0.75}\left(\frac{1}{1+\left(\frac{PMA}{TM_{50}}\right)^{-Hill_{CL}}}\right)e^{\eta_k}$$

(Eq. 2)

The determination of adding other covariate effects was judged on the log-likelihood ratio test (LRT) using an automatic procedure of stepwise covariates modeling (SCM), by initializing

LRT threshold values in the "Model Building" module of Monolix. Specifically, the stepwise forward addition was carried out with the statistical criteria of log-likelihood $P < 0.05$ followed by a backward elimination process with $P < 0.01$. [40] The age effects on other PK parameters were modeled with a power law relationship normalized to 30 years. In Equation 3, θ denotes the population parameters, and η denotes the random effects).

$$COV = logt_{AGE} = \log\left(\frac{AGE}{30}\right)$$

$$\log(\theta_i) = \log(\theta_{pop}) + \beta_{COV} \times COV + \eta$$

$$\theta_i = \theta_{pop} \times \left(\frac{AGE}{30}\right)^{\beta_{COV}} \times e^{\eta}$$

(Eq. 3)

The dichotomous CATs were modeled with exponential function coded with zero for a dosage of 6 mg as well as the IM route (the reference group) and one for a high dosage of 12 mg as well as IN route (Eq.4). Considering the mechanic plausibility, we only assessed the route effect on diamorphine absorption.

$$CAT_1 = 0, \text{if route} = \text{IM};\ CAT_1 = 1, \text{if route} = \text{IN}$$

$$CAT_2 = 0, \text{if dosage} = 6\text{mg};\ CAT_2 = 1, \text{if dosage} = 12\text{mg}$$

$$\log(\theta_i) = \log(\theta_{pop}) + \beta_{CAT} + \eta$$

$$\theta_i = \theta_{pop} \times e^{\beta_{CAT}} \times e^{\eta}$$

(Eq.4)

Following a similar approach as for the covariates search, significant correlations between random effects were added to the model according to the Pearson correlation tests. Finally, the appropriate error models were applied to fit residual unexplained variability (RUV) between observations and individual predictions for each drug.

2.4 Model Evaluation

2.4.1 Internal Validation

The goodness-of-fit (GOF) for structural modeling was assessed based on the drop in corrected Bayesian information criteria (dBICc), which are derived from the objective function value (OFV) expressed as –2 × log-likelihood. Graphical evaluations include GOF diagnostic plots such as model-predicted population (PRED) and individual concentration (IPRED) versus observed concentration (OBS) and density distribution of the normalized population (NPDE) as well as individual weighted residuals (IWRES). During the expropriative modeling process, model selection criteria to assess overall fit were guided by the following aspects: the mechanistic plausibility and utility, the drop in BICc for non-nested models, the minimum OFV determined via importance sampling for nested models, the visual diagnostics plots, and the precision of parameter estimates judged by %RSE.[41]

The predictive performance of the final pop-PK models was evaluated by visual predictive check (VPC) plots constructed by 1000 simulations derived from the original index dataset. To reduce the impact of areas with sparse data, the observed and simulated PK data were automatically grouped in multiple bins over successive time intervals based on the optimized least-

squares binning criteria.[42] Additionally, we reported the shrinkage for the distribution of the individual PK parameters.

2.4.2 External Validation

The robustness of model extrapolation was also assessed by external verification of observed and predicted PK parameters in adults after IM dosing [32] and children after IN dosing [33]. The intranasal administrations were simulated with 5 replicates for 1000 virtual subjects at the same time point sampled in clinical studies using the population parameters (both fixed and random effects including covariates) estimated by Monolix. The span of ages and body weights for the virtual adult population (24-39 years, 43-85 kg) and virtual pediatric population (4-13 years, 19-59 kg) were restricted to the range of PK study participants who contributed to the measured data. Given the developmental relationship between age and body weight in children, all virtual pediatric subjects were created using the Simcyp® simulator (v22, Certara) population module. Morphine exposures (area under the plasma concentration-time curve; AUC) were computed by integrating the concentration profile from the start to the end of the observation period (Appendix A)

The fold-error (observed/predicted ratio, $R_{pred/obs}$) and average fold error (AFE) of morphine C_{max} and $AUC_{0\text{-}t}$ were calculated (Eq.5). A two-fold error range (within 0.5−2-fold range) was used for the evaluating $R_{pred/obs}$ for PK parameters. [43]

$$ratio_{\left(\frac{pred}{obs}\right)} = \frac{\text{Predicted PK parameter}}{\text{Observed PK parameter}}$$

$$AFE = 10^{\frac{\sum \log(fold\ error)}{N}}$$

(Eq.5)

Additionally, for the pediatric simulation, we also assessed the mean plasma concentration-time profile of morphine observed within 1 hour from children administered with IND 0.1 mg/kg. To match the PK sampling time point, the morphine concentrations were simulated at 0.033, 0.087, 0.167, 0.25, 0.5, and 1 hour.

2.5 Dosing Regimen Simulations

An adult population (18-65 years), as well as four representative pediatric populations, were created using the Simcyp® simulator (v22, Certara) population module to match the FDA Pediatrics Exclusivity Study Age Groups (baby infants: 1 month – 6 month, infants: 1 month – 2 years, children: 2 – 12 years and adolescents: 12 – 16 years).[44] The morphine concentration-time curves for 12 hours were simulated with 5 replicates in 5000 virtual pediatric subjects (1000 subjects per age group). The subjects were generated based on the default Caucasian population, with the female proportion setting of 0. To mimic the clinical usage of injectable diamorphine for acute pain, three doses of intranasal diamorphine were repeated every four hours. Simulations from the developed Pop-PK model were used to devise an optimal pediatric intranasal dosing scheme that targeted comparable morphine exposures ($AUC_{0\text{-}t}$) and the steady-state maximum concentrations ($C_{ss,\,max}$) to healthy adults.

3.0 Results

3.1 Study Subjects Characteristics

For this analysis, PK data were collected from 10 male volunteers with a history of heroin use, resulting in a total of 385 observations across 28 treatment sessions. **Table 2** provided the overall demographic information for each treatment group. The treatment of 6 mg dosing of diamorphine accounts for 71.4% representing 0.07–0.09 mg/kg which is close to the clinical usage of diamorphine hydrochloride nasal spray (freeze-dried powder, Ayendi) in breakthrough pain. Besides, all subjects received a minimum of three consecutive days of negative tests to assure they are opioid-free.

Table 2. Characteristics of study subjects for pop-PK analysis.

Treatment Group	IN 6 mg	IN 12 mg	IM 6 mg
No. of Subjects (%)	10 (35.7%)	10 (35.7%)	8 (28.6%)
Weight (kg)	72.16 [60.4-81.4]	72.16 [60.4-81.4]	73.19 [60.4-81.4]
Age (years)	31.38 [23-41]	31.38 [23-41]	28.25 [23-41]
Sex	Male	Male	Male
$CAT_1 = 1$	0	10 (35.7%)	0
$CAT_2 = 1$	20 (35.7%)		0

Continuous variables are given as median (range), and categorical variables as number (percent). The influence of dosage amounts (CAT_1) and administration route (CAT_2) were tested in the stepwise covariates modeling. IM, intramuscualr rote group, IN, intranasal route group.

3.2 Pop-PK Model Development

3.2.1 Structure Modeling Results

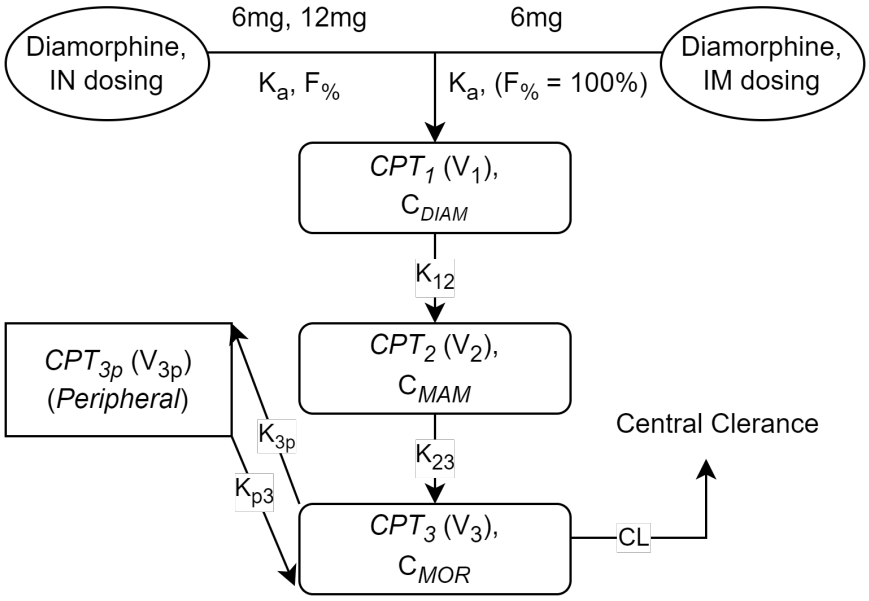

Figure 2 Schematic representation of the final pharmacokinetic model of diamorphine (DIAM), 6-monoacetylmorphine (MAM), and morphine (MOR). Abbreviation: CPT, compartment; IM, intramuscular route. IN, intranasal route; C, drug concentration; V1-V3, the central volumes, which were coded as V2=V1; K, the intercompartmental transfer rate constants.

A schematic representation of the final PK structural model was presented in **Figure 2**. The concentration-time profiles DIAM and MAM were best described with the one-compartment model (CPT_1 and CPT_2) while the MOR data fitted better with the two-compartment model (CPT_3 and CPT_{3p}). For the parametrization of unidentifiable central volume for metabolites, the inclusion of only morphine central volume (V_3) attained the minimum BICc. This four-compartment sequential PK disposition model thus assumed the MAM central volume was equal to diamorphine

volume (V_1 = V_2). The straightforward first-order absorption model without lag time was demonstrated as best fitting for both IND and IMD. When we separately estimated the absorption rate constant (K_a) for the two administration routes, there were minor differences, and the estimation of a common K_a improved the model fit. Transit models for absorption and metabolite formation were also investigated but did not improve the model fit with minor differences in BICc. Attempts to fit a more complex model, such as the six-compartment model utilized by Rook et al., yielded poor estimation or unstable convergence.[28]

As body weight is a size scaler that is presumed to affect all PK parameters, it was incorporated into our base model through a nested allometric scaling function. The theory-based allometric relationships of rate constant, clearance, and volume were characterized using the fixed exponents on standardized 70 kg WT with -0.25, 0.75, and 1, respectively. Although the allometric scaling model with WT only led to a trivial improvement of the model fit (dBICc = 2.3), its primary objective was to prepare the model for extrapolation to the pediatric population. Estimation of the allometric exponents worsen fitting results, as the precision of parameter estimation decreased. Meanwhile, to incorporate developmental changes associated with age, morphine clearance was combined with a well-established maturation function.

3.2.2 Statistical Modeling Results

The automatic stepwise covariates modeling did not identify other significant covariate effects. This suggested diamorphine absorption and disposition were not dosage dependent, which confirmed the mechanistic plausibility of our model structure with linear kinetics. It also revealed that the absorption constant rate is not influenced by administration route (CAT_2) . The parameterization of between-occasion variability (BOV) within each volunteer resulted in either

unsuccessful minimization or highly imprecise parameter estimates. Thus, for random effects, each treatment session was assumed to represent one "model subject" to only assess between-subject variability (BSV). Moreover, the introduction of a correlation coefficient between random effects for K_a and V_1 greatly improved the model performance (dBICc = 10.8). The most effective way to account for residual unexplained variability (RUV) in observed plasma concentration was through the use of proportional residual error models, which effectively captured assay variability and errors in sample timing.

3.2.3 Parameter Estimates Results

All population estimates of our final model are presented in **Table 3**, indicating that parameter precisions were generally acceptable with %RSE < 30% for fixed effects and %RSE < 50% for random effects. The individual variability was supported for all PK parameters by our model to evaluate the BSV in diamorphine PK. The final model estimated the relative bioavailability for IND as 52% (IQR: 50%-59%) compared to IMD, with an absorption half-life of approximately 13.7 minutes. The population parameter variabilities for K_a (BSV = 0.61) and diamorphine volumes (BSV = 0.48) are still considerable despite the inclusion of their positive correlation (corr_V_1_K_a) as well as the allometric scaling of WT. A relatively high BSV was associated with bioavailability for IND absorption (BSV = 0.57) but no covariates available were found to explain this. The estimated metabolic transfer rate constant (K_{12}) of diamorphine was found to be similar to that of 6-monoacetylmorphine (K_{23}), with both exceeding 100 h^{-1}, indicating rapid elimination from the central compartment, which represents plasma and highly perfused tissues.

Table 3. Population Pharmacokinetic parameter estimates.

PK Parameters [units]	Estimation (RSE%)	BSV (RSE%)	Shrinkage (%)	Median [IQR]
K_a [h^{-1} per 70 kg]	3.04 (12.9)	0.609 (16.1)	- 1.85	3.70 [1.67-4.63]
$F_{\%}$ [per 70 kg]	0.519 (13.6)	0.568 (27.2)	- 3.55	0.532 [0.504-0.592]
V_1 [L/per 70 kg] (=V_2)	8.21 (28.9)	0.478 (21.8)	1.33	9.43 [5.17-12.5]
V_3 [L/per 70 kg]	32.5 (13.5)	0.279 (33.5)	2.84	34.3 [29.8-38.7]
K_{12} [h^{-1}/per 70 kg]	103 (23.5)	0.400 (30.9)	- 7.19	102 [83.6-127]
K_{23} [h^{-1}/per 70 kg]	106 (23.3)	0.295 (30.1)	- 10.6	100 [91.6-115]
K_{3p} [h^{-1}/per 70 kg]	24.2 (14.1)	- 0.448		23.9 [23.3-24.6]
K_{p3} [h^{-1}/per 70 kg]	2.69 (14.3)	0.385 (29.6)	- 9.00	3.07 [2.14-3.42]
CL [L/h/per 70 kg]	132 (19.0)	0.297 (36.7)	- 9.98	139 [123-164]
corr_V_1_K_a	0.854 (23.7)			
RUV$_1$	0.430 (12.0)			
RUV$_2$	0.215 (8.34)			
RUV$_3$	0.236 (6.74)			

Median and interquartile range (IQR) and shrinkage were computed from conditional distribution using Monolix default Markov chain Monte Carlo (MCMC) convergence assessment. The relative standard error (RSE) was obtained from the Fisher Information Matrix via stochastic approximation. Fixed effects of parameter estimates and random effects of between-subject variability (BSV) were computed using the Stochastic Approximation Expectation-Maximization (SAEM) algorithm.

Abbreviations: K, intercompartment rate constant. V, central compartment volume. $F_{\%}$, bioavailability for intranasal diamorphine. RUV, residual unexplained variability with proportional error model. DIAM, diamorphine. MAM, 6-monoacetylmorphine; MOR, morphine.

3.3 Pop-PK Model Evaluation

3.3.1 Internal Validation

Diagnostic goodness-of-fit plots (**Figure 3**) for the population predictions (PRED) versus observations (OBS) indicated that there is no major bias in the population component. Likewise, individual predictions (IPRED) versus OBS demonstrated that the structural model should be useful to the majority of individuals with less than 10% of outliers in our final model. In **Figure 4**, the comparison between the empirical residual distribution and the theoretical Gaussian distribution shows a good overlay, indicating no significant misspecification in our structural and residual error models. Noticeably, the conditional distribution was utilized to obtain random samples for IPRED and IWRED graphical diagnostics, as well as shrinkage computation for individual parameters (**Table 3**), to circumvent the potential bias in the original data. The low shrinkage demonstrated the individual parameters (EBEs) were precisely estimated.

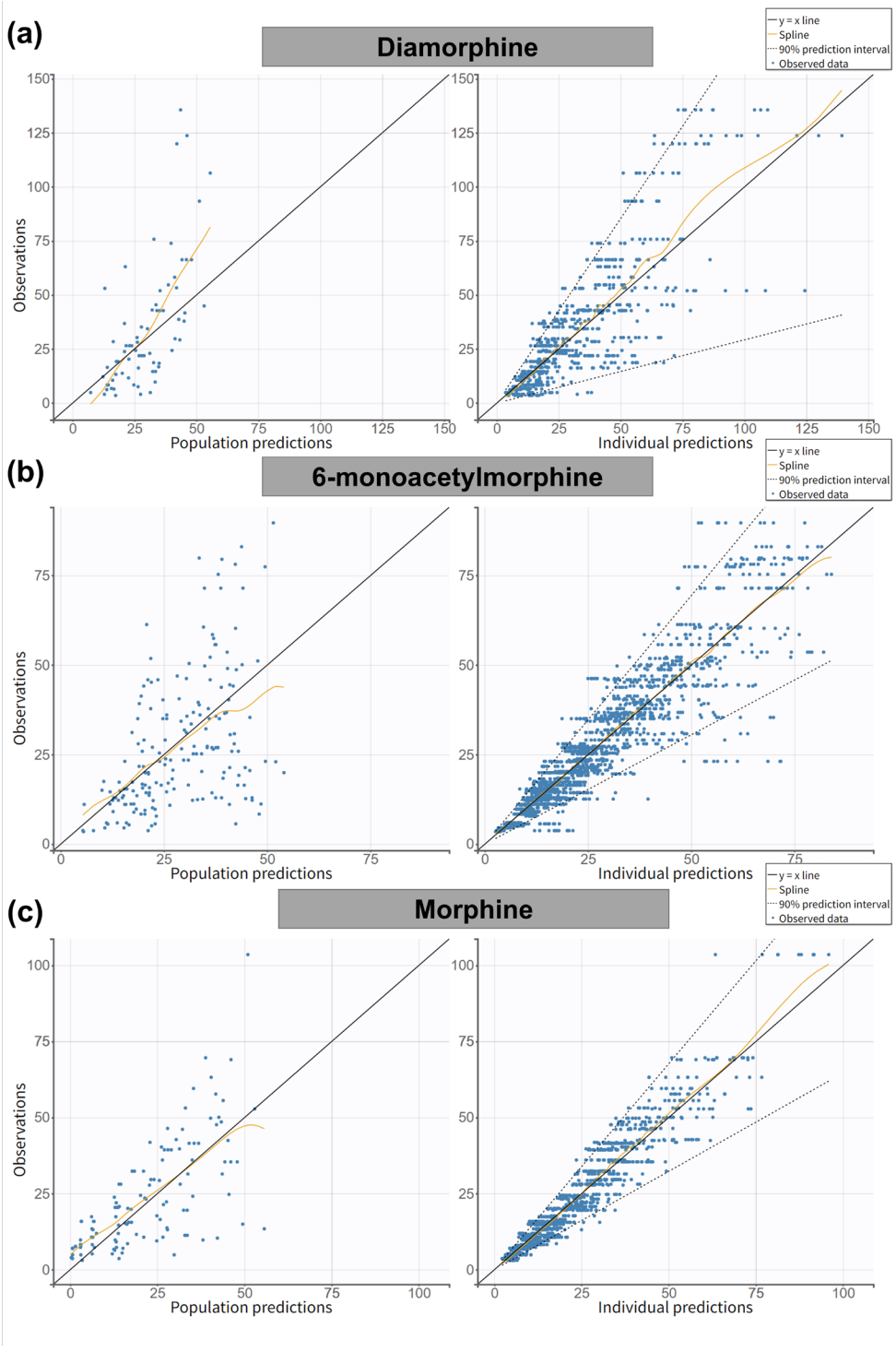

Figure 3. Assessment of the structural model by predictions versus observationsfor population (left) and individual (right) model for diamorphine (a), 6-monoacetylmorphine (b), and morphine concentration (c). The individual model is based on conditional distribution.

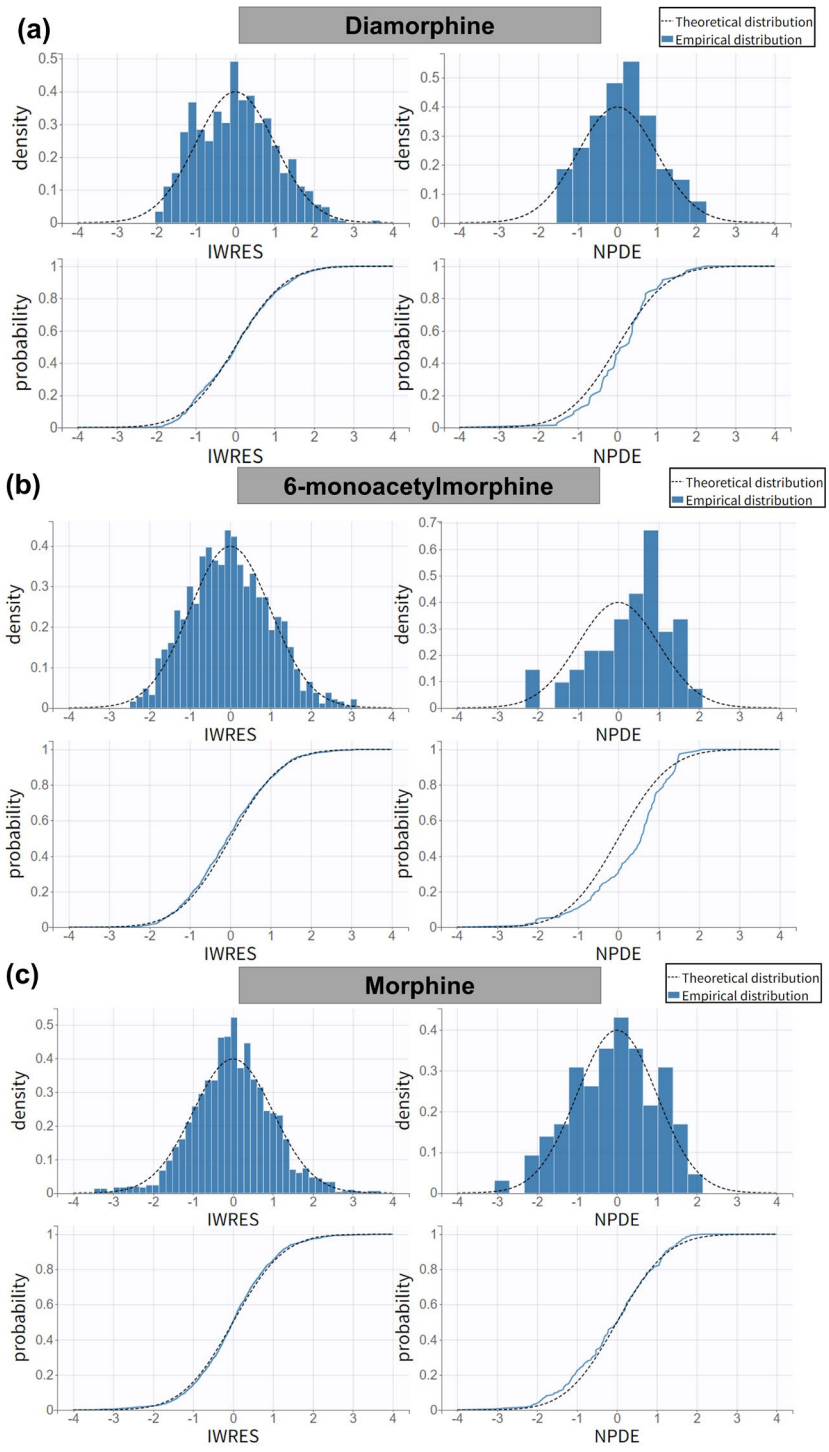

Figure 4. The empirical distribution plots of the residuals including the IWRES (left), and the NPDEs (right) using cumulative distribution function (CDF, below) and probability density function (PDF, upper) for diamorphine **(a)**, 6-monoacetylmorphine **(b),** and morphine concentration **(c)**. IWRES, individual weighted residuals. NPDE, normalized prediction distribution errors.

Figure 5 displays the prediction-corrected visual predictive checks (pc-VPC), which indicate that our sequential pop-PK model provides a reasonable prediction for observed DIAM, MAM, and MOR concentrations. This is demonstrated by the acceptable overlay of the median, 5th percentile, and 95th percentile of OBS within the 90% predictive intervals for the corresponding percentiles of the simulated data. Despite its overall reasonable predictive performance, the final model tended to underpredict observed diamorphine concentrations in the early sampling time bins (0-0.12h) and M6M concentrations in late time bins (0.6-1.5h), as illustrated in **Figures 5a and 5b**, respectively. Additionally, the NPDE residual distribution (empirical vs. theoretical) for MAM indicated mild misspecification, as shown in **Figure 4b**.

These limitations may be attributed to the challenge of simultaneously modeling three drug components and the limited availability of measured data to explain the high between-subject variability (BSV) observed in the two precursor drugs. Nonetheless, the model was able to accurately simulate the time course of morphine concentrations, reproducing both the central trend and variability observed in the original dataset (**Figure 5c**). Consequently, in the next stage, we only evaluated morphine concentration which is more correlated to analgesic effects.

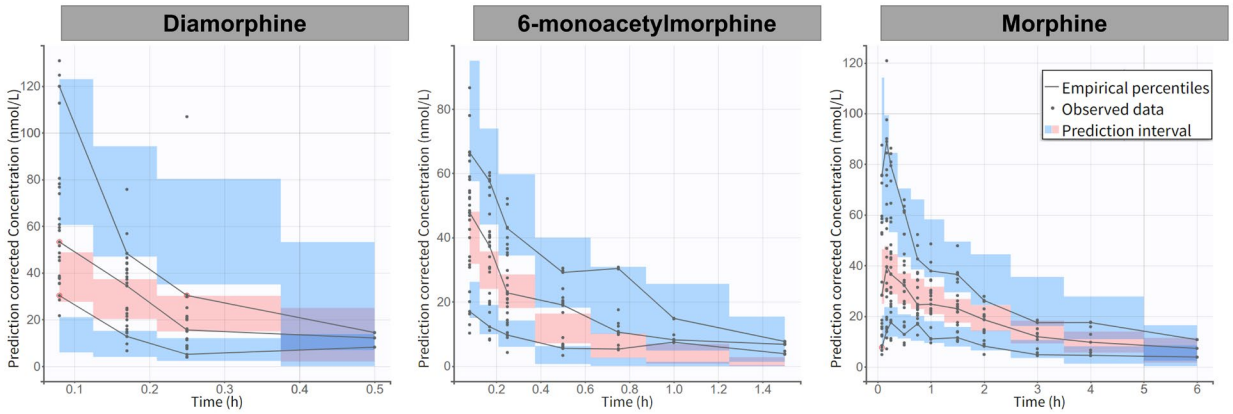

Figure 5. prediction-corrected Visual predictive checking (pc-VPC) plots for diamorphine (a), 6-monoacetylmorphine (b), and morphine concentration (c) of the final pop-PK models. The gray points represent the observed data of concentration in nM or nmol/L. The solid gray lines represent the 5th, 50th, and 95th of empirical percentiles for the observations. The shaded areas represent the 90% confidence (predictive) interval of the 5th, 50th (reddish color), and 95th percentiles of the simulated data.

3.3.2 External Validation

Table 4 presents the observed and predicted PK parameters of external datasets consisting of 4 treatment schemes. All PK parameters were predicted within the two-fold error range, showing acceptable prediction with average fold errors of 0.95 (range: 0.70-1.31) for C_{max} and 0.80 (range: 0.71-0.91) for $AUC_{0\text{-}t}$. In addition, the validity of the model extrapolation was further confirmed by the VPC shown in **Figure 6**, which demonstrates successful prediction of morphine time-concentration profile within 1 hour in children aged 4-13 years following intranasal dosing with 0.1 mg/kg in the A&E department.

Table 4. Observed and predicted PK parameters.

Dose	C_{max} (µmol/L)			AUC_{0-t} (µmol.min/L)		
	Observed	Predicted	$R_{pred/obs}$	Observed	Predicted	$R_{pred/obs}$
IMD, Adults [32]						
181 µmol	1.1	0.767	0.70	120	91.60	0.76
366 µmol	1.7	1.58	0.93	224	185.3	0.83
548 µmol	1.7	2.22	1.31	305	277.4	0.91
IND, Children [33]						
0.1 mg/kg	0.0361	0.0353	0.98	1.794	1.265	0.71
Average Fold Errors (AFE)						
		0.95			0.80	

The observed PK parameters are the mean values from 6 adult subjects injected with intramuscular diamorphine (IMD) and the median value from 12 pediatric subjects treated with intranasal diamorphine (IND). The predicted values were obtained accordingly under 5 simulations to calculate the fold errors (observed/predicted ratio, $R_{pred/obs}$).

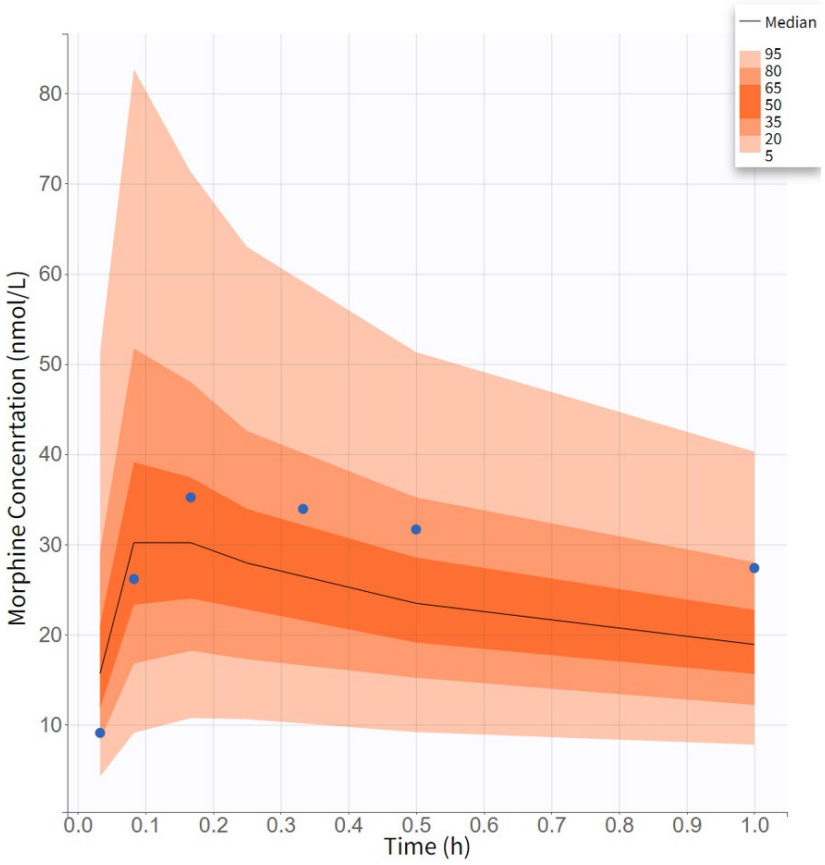

Figure 6. Visual predictive checking (VPC) using pediatric data. The solid blue point represents the mean observation from children extracted from Kidd. et al. [33] The solid black line represents the simulated median concentration. The shaded orange area represents a 95% prediction interval.

3.4 PK-guided Dose Optimizations

The boxplots in **Figure 7a** compared simulated morphine $AUC_{0\text{-}12h}$ in 5000 virtual subjects across 5 age groups receiving the current diamorphine weight-normalized dose (0.1 mg/kg). The median exposures of the reference adult group ($AUC_{0\text{-}12h}$) achieved 75 µg.h/L (IQR: 56.8-89.6 µg.h/L) which is concordant with the 70 µg.h/L ($AUC_{0\text{-}10h}$) reported by Morse et. al. [23] In general,

all pediatric median exposures fell within the interquartile range (IQR) of referenced adult exposures. However, a statistical difference in pediatric median exposures was observed when compared to the referenced exposures based on 5 simulations. Specifically, the baby infants achieved higher $AUC_{0\text{-}12h}$ values while other age groups did not achieve the referenced exposure level (**Figure 7a**).

Therefore, we proposed a new dosage regimen of IND for each age group to target a similar exposure level, as summarized in **Table 5**. Application of this optimal dosing strategy towards the same study subjects resulted in the pediatric median exposures comparable to the adults, as shown in **Figure 7b** (median differences < 2 μg.h/L). The optimized dosing regimen also led to more than 90% of children achieving therapeutic window $C_{ss,\ max}$ between 10-20 μg/L to exhibit analgesic effects.

Table 5. Optimal dosage scheme and characteristics of virtual populations.

Group	Baby infants (BINF)	Infants (INF)	Children (CHI)	Adolescents (ADO)	Referenced Adults (REF)
Postnasal Age	1 – 6 month	6 month – 2 years	2 – 12 years	12 – 18 years	18 – 65 years
Body Weight (kg)	5.8 (4.8 – 6.8)	11.13 (9.5 – 12.9)	22.3 (17.7 – 28.6)	27.6 (18.5 – 44.9)	80.2 (71.6 – 88.8)
IND Dosage (mg/kg)	0.085	0.125	0.125	0.120	0.100

Representative virtual subjects across different age bands was created in Simcyp (Certara, v22) Population Module. The pediatric dosing was optimized to target comparable morphine exposures to adults. Weight is given as the median (interquartile range). IND, intranasal diamorphine.

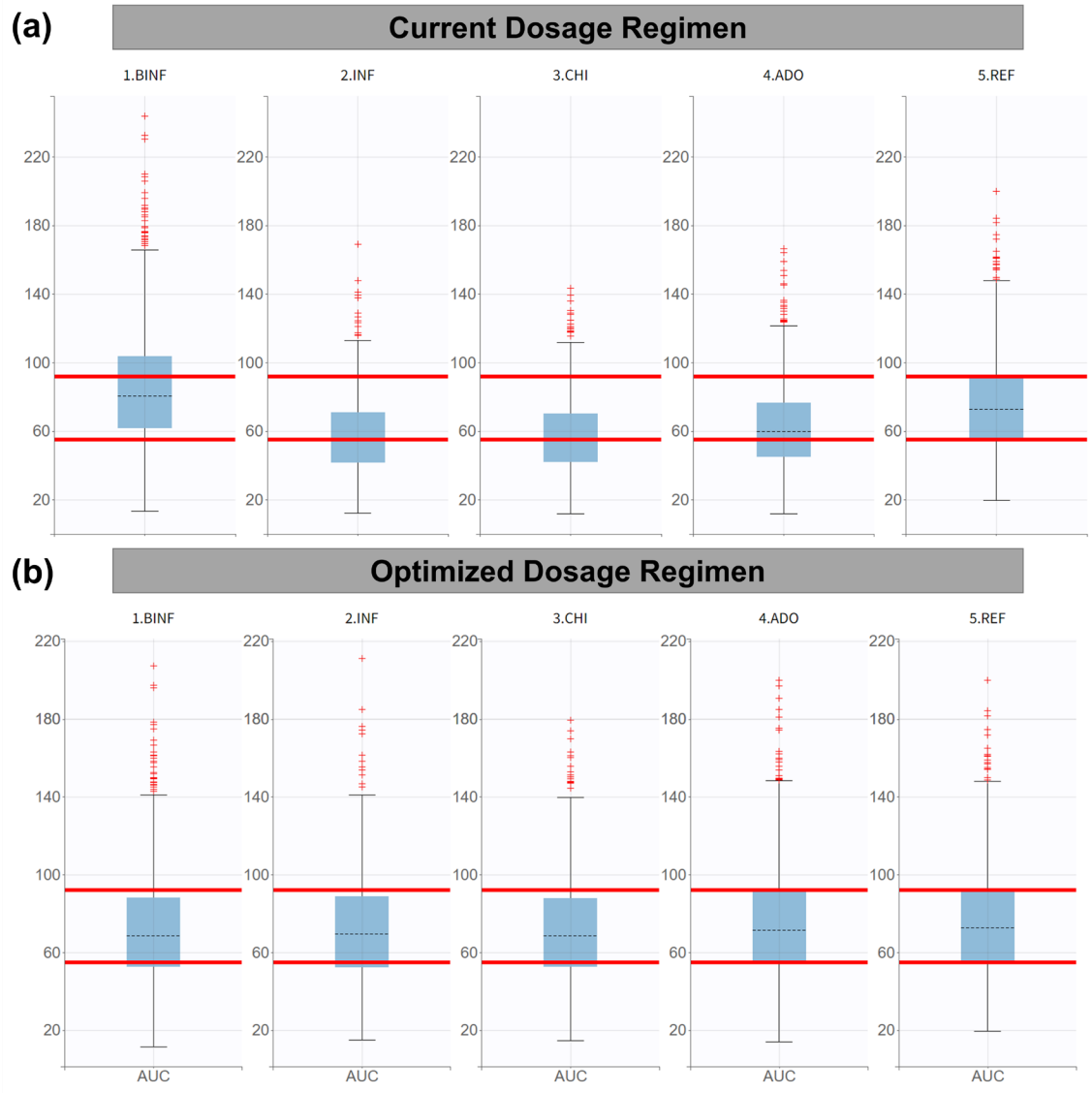

Figure 7. The comparison of simulated morphine exposureunder the current dosage regimen (a) and the optimized dosage strategy proposed in this study (b). The solid red line represents the interquartile range of referenced adult exposures treated with weighted-standardized dosage (0.1 mg/kg IND). The boxplots of simulated $AUC_{0\text{-}12h}$ were computed for 1000 virtual subjects for each age group in Table 5 (BINF, baby infants, INF, infants, CHI, children, ADO, adolescents, REF, referenced adu

lts).

4.0 Discussion

In this study, we collected and analyzed the publicly available Pharmacokinetics data in subjects receiving low-dosage diamorphine across two routes of administration (IM and IN) over a twofold range of doses. An integrated pop-PK model was developed to describe the concentration-time profiles of diamorphine, 6-monoacetylmorphine, and morphine. The external verification by the average fold errors of PK parameters as well as C-T profiles supported the predictive utility of model extrapolation. Optimal pediatric dosages were derived using a simulation-based and PK-guided methodology for four broadly representative pediatric populations across different age groups.

4.1 The usefulness of our Pop-PK model

The PKs of diamorphine, 6-monoacetylmorphine, and morphine were best captured by a joint four-compartment linear model. The model estimated the IND relative bioavailability to be ~ 52% (95% CI: 50%-59.2%) and uncovered a similar first-order absorption behavior for IM injection and IN delivery with 13.6 min of absorption half-life. This agreed with the reported 50% bioavailability according to traditional non-compartmental analysis. [29,31,33] The addition of categorical covariate of administration route (CAT_2) on the weight-normalized absorption rate constant (K_a) did not lead to a statistically significant difference in model fit. Nonetheless, a high BSV was associated with K_a, which might explain the underprediction observed in the early

absorption phase shown by VPC inspection (**Figure 5a**). Identification of additional sources of unknown variability can future improve the predictive performance of the current model.

Previous research suggested that (acetyl)-metabolites are barely recovered in the urine and morphine and its glucuronide metabolites of M3G and M6G are the major detectable forms. [45-47] This explains the reason why we discarded the renal excretion of DIAM and MAM and we assumed their central volumes are equal. The intermediate metabolite, MAM, is not directly administered and any combination of biotransformation rate (K_{12} and K_{23}) in the model structure is sufficient to fit PK data. Thus, the estimation of unidentifiable MAM volumes (V_2) would pose a challenge to model fitting as any change in superfluous V_2 can be offset by adjusting other parameters.

The possibility of saturation of metabolism was not considered due to the widespread distribution of various esterases that are abundant in the human body. Besides, the administration of a small dose of diamorphine is less likely to result in saturation metabolism. Therefore, our model described a mono-exponential decline of rapidly metabolized precursors (DIAM and MAM) observed in concentration-time curves. The estimated metabolic conversion half-life for deacetylation was 0.4 minutes. It refers to the biotransformation rate by hydrolysis that occurs in the central circulatory system and is carried out by the butyrylcholinesterase (BChE) in erythrocytes and human carboxylesterase (hCES) in hepatocytes (**Figure 1**).[48] [49] These enzymes are fully functional at birth, and thus no maturation function is required.[23] Rook et. al employed a two-compartment model to estimate a system biotransformation half-life (~2-4 min) in both central and peripheral tissues. [28] Intriguingly, this is consistent with the findings of Salmon et. al [49] and Kim et. al [50] that BChE and hCES are the primary perpetrators of diamorphine deacetylation. In other words, the peripheral esterase might represent a slow-

metabolizing enzyme in the context of diamorphine deacetylation. Moreover, no significant relationship between dosage amount and the PK parameters was found, indicating that the structure design of linear kinetics should be reasonable mathematically and mechanically. However, the current "dosage-independent" finding is only feasible for the diamorphine usages of low dosage, as the available data is limited.

Albeit we incorporated reported population PK parameters of diamorphine and morphine as prior information using the Bayesian approach, the final model presented some differences in estimated values compared to the only published pop-PK analysis of diamorphine [28]. Attempts to fix parts of population estimates did not improve model fit and generate less reliable estimates. It is possible that the discrepancies stem from differences in model structure, quantification limits based on varying analytical methods (GC/MS vs. LC-MS/MS), and vastly different dosage amounts of the study medication used (with a dosage ratio of 10-50 times). It is still worth noting that our model is more applicable to the medical use of intranasal diamorphine for pain management, rather than the heroin-assisted treatment prescribed for opioid addicts, which requires much larger dosing. Furthermore, the state-of-the-art SAEM algorithm we adopted is superior to the traditional first-order approaches, like FOCE-I (First-order conditional estimation with interaction) which is of concern to generating biased estimates of random effects. [41]

All typical values of PK parameters of the final model are standardized by WT 70 kg whilst a model capturing the maturation of renal function was used to characterize the overall clearance of the morphine.[39] Our estimated morphine central volumes (32.5 L) are consistent with reported population estimates (46.8 L) [51]. The seemingly high estimated values of CL (132 L/h) represented the sum of hepatic and renal elimination, which is also concordant with the apparent clearance reported in children. [39] Moreover, the external verification confirmed the usefulness

to predict important PK parameters when extrapolating our model to population outside the study group (from adults to children) and outside the study dosing (from low to high dosage). Particularly, the simulated morphine concentration-time profile closely resembled the observed clinical data from children given by IND dosing 0.1 mg/kg [33]. This provides additional evidence of the utility of our model in PK prediction for pediatric breakthrough pain management.

4.2 Simulation-based and PK-guided dosage optimization

The area under the curve (AUC) is a commonly used metric to determine the optimal pediatric dosage, as it is directly correlated with the average concentration level over the exposure period. This approach has been applied to guide pediatric dosing for various drugs, including nalbuphine[52], vancomycin[53], olanzapine[54], and metoclopramide[55], etc. The current intranasal diamorphine dose regimen of 0.1 mg/kg resulted in a significant difference in morphine AUC_{0-t} observed in all age groups compared to the adult group. Simulation by single intranasal diamorphine was then used to target comparable morphine exposures in all age groups. The utilization of model-based simulation methodology to investigate the dose-exposure-response relationship is favored by drug regulatory bodies. Thus, we recommended an initial dose of 0.12-0.125 mg/kg for infants, children, and adolescents, and a lower initial dose of 0.085 mg/kg for infants under one month of age. The dose titration process should be carried out based on the changing experience of pain and analgesia in children.

The dosages recommended by the optimized dosing strategy (**Table 6**) were found to be concordant with the standard of care used in the Emergency Department, ranging from 0.1 mg/kg with a 20% variability. [11] However, due to the unknown nasal anatomy development in infants,

the intranasal dosage prediction for this age group remains speculative, and further research is warranted. Morse et al. developed an age-related dosage strategy for children, but they only utilized established population compartment models with a scaling and maturation function. [23] We developed a new pop-PK model using the IND data, which allowed us to estimate the previously unknown intranasal absorption parameter (K_a, $F_{\%}$) and updated other PK disposition parameters. Our modeling work enabled us to introduce reasonable individual parameter distributions with small shrinkage values to yield confident predictions of the concentration-time curves. Furthermore, the virtual pediatric populations we created have a range of weights and ages, instead of the representative with standard covariates, to better replicate real-world conditions for conducting clinical simulations.

4.3 Limitations and Future

Our study has several limitations. First, females were excluded from the pharmacometrics analysis, which may limit the generalizability of our findings. This exclusion was due to the biased recruitment of study participants for PK data collection, and future studies should aim to recruit a more representative sample. Additionally, the limited PK data and missing clinically relevant covariates such as genotype information of esterase and concomitant drug usage may have reduced the power and ability to detect covariate relationships. This could have contributed to the high BSV estimates of some population parameters (K_a, K_{12}, and V_1) and the anticipated bias in the predicted concentrations of two morphine precursors. Thirdly, the current model did not include the morphine metabolites, which could have led to an overestimated morphine central clearance and corresponding underpredicted exposures, as shown by the low $R_{pred/obs}$ of AUC_{0-t} (**Table 4**).

Integration of PK data of M3G and M6G metabolites in future studies could extend the model and improve the understanding of the maturation relationship between renal clearance and age.

Albeit these limitations, the existing population models did not reveal the significant impacts of sex and cocaine or alcohol abuse on diamorphine PK. [28] Also, our model was able to simulate the expected dose-exposure relationship in the target population, as confirmed by external evaluation, despite the limited sample size of the model development dataset.

Lastly, it should be noted that the proposed dosage adjustment based solely on body weight and age may not fully capture the dynamic changes in organ maturation rates, blood flow, body composition, and the ontogeny of drug elimination and transport mechanisms. Physiologically based pharmacokinetic (PBPK) models can provide a more mechanistic framework that considers these factors and enable a more rational extrapolation across different pediatric age groups. [56] Nevertheless, the current study offers an initial exploration based on observed clinical PK information, which translates data into knowledge with respect to diamorphine nasal spray and characterized the relevant statistical elements for further assessment. Our pharmacometric analysis kept the mind of developing useful models that are “fit-for-purpose” to provide insights into optimal dosage selection.

In next stage, integration of more preclinical PK information (e.g., *in vitro* hCES kinetics) and clinical PD data (e.g., pupillometry and pain scores) into PBPK modeling would be beneficial. Meanwhile, as part of the "Learn and Confirm" cycle in drug development following clinical trial simulations [57], future studies into diamorphine can be designed in fewer children to confirm or improve the uncertain aspects of the current model using a sparse sampling technique to quantify important metabolites. This approach could help minimize the potential harm and further optimize

the dosing strategy for different pediatric age groups and improve the accuracy of predictions made by the model.

5.0 Conclusions

Overall, the developed pop-PK model provided valuable insights into the pharmacokinetics of diamorphine, 6-monoacetylmorphine, and morphine in adults following intranasal administration. The utilization of population modeling has enhanced the estimation of parameters and variability by identifying covariates that contribute to the variability. Specially, the pharmacometrics analysis indicated that the relative bioavailability of intranasal diamorphine is approximately 50% compared to intramuscular delivery with a similar absorption mode. Moreover, our model was found to be applicable in extrapolating to children based on body weight allometry and renal function maturation, as confirmed by external evaluation. Finally, the simulation from the final model was used to develop an optimal weight-based dosage regimen for children of different ages. This dosing scheme could serve as a useful guide for the development of future safety and efficacy studies to promote the appropriate use of intranasal diamorphine in children with breakthrough pain.

Appendix A Mlxtran code for final pop-PK model

```
[POPULATION]
DEFINITION: ;;; Prior information using Bayesian Method
F_pop = {distribution=logitNormal, typical=0.5, sd=1}
V1_pop = {distribution=logNormal, typical=58.8, sd=1}
CL_pop = {distribution=logNormal, typical=71.05, sd=1}
V3_pop = {distribution=logNormal, typical=136, sd=1}

[COVARIATE]
input = {AGE, WT}

EQUATION:
logtWT = log(WT/70)
logtWT_0 = log((WT/70)^-0.25)
PMA = 40+AGE*52
Maturation = log(1/(1+(58.1/PMA)^3.58))
logtWT_1 = log((WT/70)^0.75)

[INDIVIDUAL]
input = {V1_pop, omega_V1, k12_pop, omega_k12, k23_pop, omega_k23, k34_pop, omega_k34, k43_pop,
omega_k43, ka1_pop, omega_ka1, F_pop, omega_F, logtWT, beta_V1_logtWT, logtWT_0, beta_k43_logtWT_0,
beta_k34_logtWT_0, beta_k23_logtWT_0, beta_k12_logtWT_0, beta_ka1_logtWT_0, corr_ka1_V1, CL_pop,
omega_CL, Maturation, beta_CL_Maturation, logtWT_1, beta_CL_logtWT_1, V3_pop, omega_V3,
beta_V3_logtWT}

DEFINITION:
```

V1 = {distribution=logNormal, typical=V1_pop, covariate=logtWT, coefficient=beta_V1_logtWT, sd=omega_V1}

k12 = {distribution=logNormal, typical=k12_pop, covariate=logtWT_0, coefficient=beta_k12_logtWT_0, sd=omega_k12}

k23 = {distribution=logNormal, typical=k23_pop, covariate=logtWT_0, coefficient=beta_k23_logtWT_0, sd=omega_k23}

k34 = {distribution=logNormal, typical=k34_pop, covariate=logtWT_0, coefficient=beta_k34_logtWT_0, sd=omega_k34}

k43 = {distribution=logNormal, typical=k43_pop, covariate=logtWT_0, coefficient=beta_k43_logtWT_0, sd=omega_k43}

ka1 = {distribution=logNormal, typical=ka1_pop, covariate=logtWT_0, coefficient=beta_ka1_logtWT_0, sd=omega_ka1}

F = {distribution=logitNormal, typical=F_pop, sd=omega_F}

CL = {distribution=logNormal, typical=CL_pop, covariate={Maturation, logtWT_1}, coefficient={beta_CL_Maturation, beta_CL_logtWT_1}, sd=omega_CL}

V3 = {distribution=logNormal, typical=V3_pop, covariate=logtWT, coefficient=beta_V3_logtWT, sd=omega_V3}

correlation = {level=id, r(ka1, V1)=corr_ka1_V1}

[LONGITUDINAL]

input = {b1, b2, b3}

;;;

input = {ka1, F, V1, V3, k12, k23, k34, k43, CL}

PK:

depot(type = 1, target=A1, ka = ka1, p = 1) ;IM depot compartment (reference)

depot(type = 2,target=A1, ka = ka1, p = F) ;IN depot compartment

EQUATION:

;odeType = stiff

t_0 = 0

A1_0 = 0 ; A1 = amount of parent drug in central compartment

A2_0 = 0 ; A2 = amount of 6MAM in central compartment

A3_0 = 0 ; A3 = amount of MOR in central compartment

A4_0 = 0 ; A4 = amount of MOR in Peripheral compartment

k30 = CL/V3

;;; DIAM

ddt_A1 = - k12*A1

;;; 6-AM

ddt_A2 = k12*A1 - k23*A2

;;; MOR

ddt_A3 = k23*A2 + k43*A4 - k34*A3 - k30*A3

ddt_A4 = -k43*A4 + k34*A3

C1 = A1/V1

C2 = A2/V1

C3 = A3/V3

;=====;Calculation of AUC

AUC1_0 = 0

AUC2_0 = 0

AUC3_0 = 0

ddt_AUC1 = C1

ddt_AUC2 = C2

ddt_AUC3 = C3

OUTPUT:

output = {C1,C2,C3}

table={AUC1, AUC2, AUC3}

;;;;

DEFINITION:

y1 = {distribution=normal, prediction=C1, errorModel=proportional(b1)}

y2 = {distribution=normal, prediction=C2, errorModel=proportional(b2)}

y3 = {distribution=normal, prediction=C3, errorModel=proportional(b3)}

Appendix B Initial Estimates (IE) for the final pop-PK model

Table S1 Initial estimates (IE) for parameter estimation in Monolix

PK Parameters [units]	Population value (Estimation Mode)	Standard Deviation (Estimation Mode)	ETA-Distribution
K_a [h^{-1} per 70 kg]	3.27(MLE)	1 (MLE)	log-normal
$F_{\%}$ [per 70 kg]	0.49 (Bayesian, sd=1)	1 (MLE)	logit-normal
V_1 [L/per 70 kg]	9.61 (Bayesian, sd=1)	1 (MLE)	log-normal
V_3 [L/per 70 kg] (= V_2)	28.55 (Bayesian, sd=1)	1 (MLE)	log-normal
K_{12} [h^{-1}/per 70 kg]	87.55 (MLE)	1 (MLE)	log-normal
K_{23} [h^{-1}/per 70 kg]	90.42 (MLE)	1 (MLE)	log-normal
K_{3p} [h^{-1}/per 70 kg]	22.55 (MLE)	1 (MLE)	log-normal
K_{p3} [h^{-1}/per 70 kg]	2.89 (MLE)	1 (MLE)	log-normal
CL [L/h/per 70 kg]	108.45 (MLE)	1 (MLE)	log-normal
corr_V_1_K_a	0.78 (MLE)		
RUV_1	0.412(MLE)		
RUV_2	0.093 (MLE)		
RUV_3	0.237 (MLE)		

MLE, maximum likelihood estimation; Bayesian approach, maximum a posterior estimation. ETA, the random effects of population values following the distribution model with the mean (0) and corresponding standard deviation (sd), i.e., the between-subject variability (BSV).

K, intercompartment rate constant. V, central compartment volume. F%, bioavailability for intranasal diamorphine. RUV, residual unexplained variability with proportional error model. DIAM, diamorphine; MAM, 6-monoacetylmorphine; MOR, morphine.

Bibliography

1. Strang, J.; Groshkova, T.; Uchtenhagen, A.; Van Den Brink, W.; Haasen, C.; Schechter, M.T.; Lintzeris, N.; Bell, J.; Pirona, A.; Oviedo-Joekes, E.; et al. Heroin on trial: Systematic review and meta-analysis of randomised trials of diamorphine-prescribing as treatment for refractory heroin addiction. *British Journal of Psychiatry* **2015**, *207*, 5-14, doi:10.1192/bjp.bp.114.149195.

2. Jamieson, L.; Harrop, E.; Johnson, M.; Liossi, C.; Mott, C.; Oulton, K.; Skene, S.S.; Wong, I.C.; Howard, R.F. Healthcare professionals' views of the use of oral morphine and transmucosal diamorphine in the management of paediatric breakthrough pain and the feasibility of a randomised controlled trial: A focus group study (DIPPER). *Palliative Medicine* **2021**, *35*, 1118-1125, doi:10.1177/02692163211008737.

3. Harrop, E.; Liossi, C.; Jamieson, L.; Gastine, S.; Oulton, K.; Skene, S.S.; Howard, R.F.; Johnson, M.; Boyce, K.; Mitchell, L.; et al. Oral morphine versus transmucosal diamorphine for breakthrough pain in children: methods and outcomes: UK (DIPPER study) consensus. *BMJ Supportive & Palliative Care* **2021**, bmjspcare-2021-, doi:10.1136/bmjspcare-2021-003278.

4. Portenoy, R.K.; Payne, D.; Jacobsen, P. Breakthrough pain: characteristics and impact in patients with cancer pain. *Pain* **1999**, *81*, 129-134, doi:10.1016/s0304-3959(99)00006-8.

5. Friedrichsdorf, S.; Postier, A. Management of breakthrough pain in children with cancer. *Journal of Pain Research* **2014**, 117, doi:10.2147/jpr.s58862.

6. Robinson, S.L.; Rowbotham, D.J.; Smith, G. Morphine compared with diamorphine. *Anaesthesia* **1991**, *46*, 538-540, doi:10.1111/j.1365-2044.1991.tb09650.x.

7. Bourquin, D.; Lehmann, T.; Hammig, R.; Buhrer, M.; Brenneisen, R. High-performance liquid chromatographic monitoring of intravenously administered diacetylmorphine and morphine and their metabolites in human plasma. *J Chromatogr B Biomed Sci Appl* **1997**, *694*, 233-238, doi:10.1016/s0378-4347(97)00149-7.

8. Rook, E.J.; Huitema, A.D.; van den Brink, W.; van Ree, J.M.; Beijnen, J.H. Pharmacokinetics and pharmacokinetic variability of heroin and its metabolites: review of the literature. *Curr Clin Pharmacol* **2006**, *1*, 109-118, doi:10.2174/157488406775268219.

9. Dinis-Oliveira, R.J. Metabolism and metabolomics of opiates: A long way of forensic implications to unravel. *J Forensic Leg Med* **2019**, *61*, 128-140, doi:10.1016/j.jflm.2018.12.005.

10. Kendall, J.M.; Latter, V.S. Intranasal Diamorphine as an Alternative to Intramuscular Morphine. *Clin Pharmacokinet* **2003**, *42*, 501-513, doi:10.2165/00003088-200342060-00001.

11. Kendall, J.; Maconochie, I.; Wong, I.C.K.; Howard, R. A novel multipatient intranasal diamorphine spray for use in acute pain in children: pharmacovigilance data from an observational study. *Emergency Medicine Journal* **2015**, *32*, 269-273, doi:10.1136/emermed-2013-203226.

12. Kendall, J.M. Multicentre randomised controlled trial of nasal diamorphine for analgesia in children and teenagers with clinical fractures. *BMJ* **2001**, *322*, 261-265, doi:10.1136/bmj.322.7281.261.

13. Wilson, J.A.; Kendall, J.M.; Cornelius, P. Intranasal diamorphine for paediatric analgesia: assessment of safety and efficacy. *Emergency Medicine Journal* **1997**, *14*, 70-72, doi:10.1136/emj.14.2.70.

14. Gastine, S.; Morse, J.D.; Leung, M.T.; Wong, I.C.K.; Howard, R.F.; Harrop, E.; Liossi, C.; Standing, J.F.; Jassal, S.S.; Hain, R.D.; et al. Diamorphine pharmacokinetics and conversion factor estimates for intranasal diamorphine in paediatric breakthrough pain:systematic review. *BMJ Supportive & Palliative Care* **2022**, bmjspcare-2021-, doi:10.1136/bmjspcare-2021-003461.

15. Van Den Anker, J.; Reed, M.D.; Allegaert, K.; Kearns, G.L. Developmental Changes in Pharmacokinetics and Pharmacodynamics. *The Journal of Clinical Pharmacology* **2018**, *58*, S10-S25, doi:10.1002/jcph.1284.

16. Chien, J.Y.; Friedrich, S.; Heathman, M.A.; de Alwis, D.P.; Sinha, V. Pharmacokinetics/Pharmacodynamics and the stages of drug development: role of modeling and simulation. *AAPS J* **2005**, *7*, E544-559, doi:10.1208/aapsj070355.

17. Laer, S.; Barrett, J.S.; Meibohm, B. The in silico child: using simulation to guide pediatric drug development and manage pediatric pharmacotherapy. *J Clin Pharmacol* **2009**, *49*, 889-904, doi:10.1177/0091270009337513.

18. Agoram, B.M. Use of pharmacokinetic/ pharmacodynamic modelling for starting dose selection in first-in-human trials of high-risk biologics. *Br J Clin Pharmacol* **2009**, *67*, 153-160, doi:10.1111/j.1365-2125.2008.03297.x.

19. Mager, D.E.; Woo, S.; Jusko, W.J. Scaling pharmacodynamics from in vitro and preclinical animal studies to humans. *Drug Metab Pharmacokinet* **2009**, *24*, 16-24, doi:10.2133/dmpk.24.16.

20. Yu, D.K.; Bhargava, V.O.; Weir, S.J. Selection of doses for phase II clinical trials based on pharmacokinetic variability consideration. *J Clin Pharmacol* **1997**, *37*, 673-678, doi:10.1002/j.1552-4604.1997.tb04354.x.

21. Lockwood, P.A.; Cook, J.A.; Ewy, W.E.; Mandema, J.W. The use of clinical trial simulation to support dose selection: application to development of a new treatment for chronic neuropathic pain. *Pharm Res* **2003**, *20*, 1752-1759, doi:10.1023/b:pham.0000003371.32474.ee.

22. Wang, Y.; Sung, C.; Dartois, C.; Ramchandani, R.; Booth, B.P.; Rock, E.; Gobburu, J. Elucidation of relationship between tumor size and survival in non-small-cell lung cancer patients can aid early decision making in clinical drug development. *Clin Pharmacol Ther* **2009**, *86*, 167-174, doi:10.1038/clpt.2009.64.

23. Morse, J.D.; Anderson, B.J.; Gastine, S.; Wong, I.C.K.; Standing, J.F. Pharmacokinetic modeling and simulation to understand diamorphine dose‐response in neonates, children, and adolescents. *Pediatric Anesthesia* **2022**, *32*, 716-726, doi:10.1111/pan.14425.

24. Bouwmeester, N.J.; Anderson, B.J.; Tibboel, D.; Holford, N.H.G. Developmental pharmacokinetics of morphine and its metabolites in neonates, infants and young children. *British Journal of Anaesthesia* **2004**, *92*, 208-217, doi:10.1093/bja/aeh042.

25. Morse, J.D.; Cortinez, L.I.; Anderson, B.J. Pharmacokinetic Pharmacodynamic Modelling Contributions to Improve Paediatric Anaesthesia Practice. *Journal of Clinical Medicine* **2022**, *11*, 3009, doi:10.3390/jcm11113009.

26. Anderson, B.J.; Holford, N.H.G. Mechanism-Based Concepts of Size and Maturity in Pharmacokinetics. *Annual Review of Pharmacology and Toxicology* **2008**, *48*, 303-332, doi:10.1146/annurev.pharmtox.48.113006.094708.

27. Germovsek, E.; Barker, C.I.S.; Sharland, M.; Standing, J.F. Scaling clearance in paediatric pharmacokinetics: All models are wrong, which are useful? *British Journal of Clinical Pharmacology* **2017**, *83*, 777-790, doi:10.1111/bcp.13160.

28. Rook, E.J.; Huitema, A.D.R.; Van Den Brink, W.; Van Ree, J.M.; Beijnen, J.H. Population Pharmacokinetics of Heroin and its Major Metabolites. *Clin Pharmacokinet* **2006**, *45*, 401-417, doi:10.2165/00003088-200645040-00005.

29. Skopp, G.; Ganssmann, B.; Cone, E.J.; Aderjan, R. Plasma concentrations of heroin and morphine-related metabolites after intranasal and intramuscular administration. *J Anal Toxicol* **1997**, *21*, 105-111, doi:10.1093/jat/21.2.105.

30. Jenkins, A.J.; Keenan, R.M.; Henningfield, J.E.; Cone, E.J. Pharmacokinetics and pharmacodynamics of smoked heroin. *J Anal Toxicol* **1994**, *18*, 317-330, doi:10.1093/jat/18.6.317.

31. Cone, E.J.; Holicky, B.A.; Grant, T.M.; Darwin, W.D.; Goldberger, B.A. Pharmacokinetics and pharmacodynamics of intranasal "snorted" heroin. *J Anal Toxicol* **1993**, *17*, 327-337, doi:10.1093/jat/17.6.327.

32. Girardin, F. Pharmacokinetics of high doses of intramuscular and oral heroin in narcotic addicts. *Clinical Pharmacology & Therapeutics* **2003**, *74*, 341-352, doi:10.1016/s0009-9236(03)00199-1.

33. Kidd, S.; Brennan, S.; Stephen, R.; Minns, R.; Beattie, T. Comparison of morphine concentration-time profiles following intravenous and intranasal diamorphine in children. *Arch Dis Child* **2009**, *94*, 974-978, doi:10.1136/adc.2008.140194.

34. Traynard, P.; Ayral, G.; Twarogowska, M.; Chauvin, J. Efficient Pharmacokinetic Modeling Workflow With the MonolixSuite: A Case Study of Remifentanil. *CPT: Pharmacometrics & Systems Pharmacology* **2020**, *9*, 198-210, doi:10.1002/psp4.12500.

35. Han, S.; Jeon, S.; Yim, D.-S. Tips for the choice of initial estimates in NONMEM. *Transl Clin Pharmacol* **2016**, *24*, 119-123.

36. Elliott, H.W.; Parke, K.D.; Wright, J.A.; Nomof, N. Actions and metabolism of heroin administered by continuous intravenous infusion to man. *Clinical Pharmacology & Therapeutics* **1971**, *12*, 806-814, doi:10.1002/cpt1971125806.

37. Kamp, J.; Jonkman, K.; van Velzen, M.; Aarts, L.; Niesters, M.; Dahan, A.; Olofsen, E. Pharmacokinetics of ketamine and its major metabolites norketamine, hydroxynorketamine, and dehydronorketamine: a model-based analysis. *Br J Anaesth* **2020**, *125*, 750-761, doi:10.1016/j.bja.2020.06.067.

38. Zhao, X.; Venkata, S.L.; Moaddel, R.; Luckenbaugh, D.A.; Brutsche, N.E.; Ibrahim, L.; Zarate, C.A., Jr.; Mager, D.E.; Wainer, I.W. Simultaneous population pharmacokinetic modelling of ketamine and three major metabolites in patients with treatment-resistant bipolar depression. *Br J Clin Pharmacol* **2012**, *74*, 304-314, doi:10.1111/j.1365-2125.2012.04198.x.

39. Holford, N.H.G.; Ma, S.C.; Anderson, B.J. Prediction of morphine dose in humans. *Pediatric Anesthesia* **2012**, *22*, 209-222, doi:10.1111/j.1460-9592.2011.03782.x.

40. Duflot, T.; Pereira, T.; Tavolacci, M.P.; Joannidès, R.; Aubrun, F.; Lamoureux, F.; Lvovschi, V.E. Pharmacokinetic modeling of morphine and its glucuronides: Comparison of nebulization versus intravenous route in healthy volunteers. *CPT: Pharmacometrics & Systems Pharmacology* **2022**, *11*, 82-93, doi:10.1002/psp4.12735.

41. Mould, D.R.; Upton, R.N. Basic concepts in population modeling, simulation, and model-based drug development-part 2: introduction to pharmacokinetic modeling methods. *CPT Pharmacometrics Syst Pharmacol* **2013**, *2*, e38, doi:10.1038/psp.2013.14.

42. Lavielle, M.; Bleakley, K. Automatic data binning for improved visual diagnosis of pharmacometric models. *J Pharmacokinet Pharmacodyn* **2011**, *38*, 861-871, doi:10.1007/s10928-011-9223-3.

43. Rasool, M.F.; Ali, S.; Khalid, S.; Khalid, R.; Majeed, A.; Imran, I.; Saeed, H.; Usman, M.; Ali, M.; Alali, A.S.; et al. Development and evaluation of physiologically based

pharmacokinetic drug-disease models for predicting captopril pharmacokinetics in chronic diseases. *Sci Rep* **2021**, *11*, 8589, doi:10.1038/s41598-021-88154-2.

44. US Food and Drug Administration (FDA). Pediatric Exclusivity Study Age Group. . Available online: https://www.fda.gov/drugs/data-standards-manual-monographs/pediatric-exclusivity-study-age-group (accessed on March 4).

45. Cone, E.J.; Jufer, R.; Darwin, W.D.; Needleman, S.B. Forensic drug testing for opiates. VII. Urinary excretion profile of intranasal (snorted) heroin. *J Anal Toxicol* **1996**, *20*, 379-392, doi:10.1093/jat/20.6.379.

46. Yeh, S.Y.; Gorodetzky, C.W.; Mcquinn, R.L. Urinary-Excretion of Heroin and Its Metabolites in Man. *Journal of Pharmacology and Experimental Therapeutics* **1976**, *196*, 249-256.

47. Gyr, E.; Brenneisen, R.; Bourquin, D.; Lehmann, T.; Vonlanthen, D.; Hug, I. Pharmacodynamics and pharmacokinetics of intravenously, orally and rectally administered diacetylmorphine in opioid dependents, a two-patient pilot study within a heroin-assisted treatment program. *Int J Clin Pharmacol Ther* **2000**, *38*, 486-491, doi:10.5414/cpp38486.

48. Meyer, M.R.; Schutz, A.; Maurer, H.H. Contribution of human esterases to the metabolism of selected drugs of abuse. *Toxicol Lett* **2015**, *232*, 159-166, doi:10.1016/j.toxlet.2014.10.026.

49. Salmon, A.Y.; Goren, Z.; Avissar, Y.; Soreq, H. HUMAN ERYTHROCYTE BUT NOT BRAIN ACETYLCHOLINESTERASE HYDROLYSES HEROIN TO MORPHINE. *Clinical and Experimental Pharmacology and Physiology* **1999**, *26*, 596-600, doi:10.1046/j.1440-1681.1999.03090.x.

50. Kim, K.; Yao, J.; Jin, Z.; Zheng, F.; Zhan, C.G. Kinetic characterization of cholinesterases and a therapeutically valuable cocaine hydrolase for their catalytic activities against heroin and its metabolite 6-monoacetylmorphine. *Chem Biol Interact* **2018**, *293*, 107-114, doi:10.1016/j.cbi.2018.08.002.

51. Bouwmeester, N.J.; Van Den Anker, J.N.; Hop, W.C.J.; Anand, K.J.S.; Tibboel, D. Age- and therapy-related effects on morphine requirements and plasma concentrations of morphine and its metabolites in postoperative infants. *British Journal of Anaesthesia* **2003**, *90*, 642-652, doi:10.1093/bja/aeg121.

52. Pfiffner, M.; Berger-Olah, E.; Vonbach, P.; Pfister, M.; Gotta, V. Pharmacometric Analysis of Intranasal and Intravenous Nalbuphine to Optimize Pain Management in Infants. *Front Pediatr* **2022**, *10*, 837492, doi:10.3389/fped.2022.837492.

53. Mulubwa, M.; Griesel, H.A.; Mugabo, P.; Dippenaar, R.; van Wyk, L. Assessment of Vancomycin Pharmacokinetics and Dose Regimen Optimisation in Preterm Neonates. *Drugs R D* **2020**, *20*, 105-113, doi:10.1007/s40268-020-00302-7.

54. Maharaj, A.R.; Wu, H.; Zimmerman, K.O.; Autmizguine, J.; Kalra, R.; Al-Uzri, A.; Sherwin, C.M.T.; Goldstein, S.L.; Watt, K.; Erinjeri, J.; et al. Population pharmacokinetics of olanzapine in children. *Br J Clin Pharmacol* **2021**, *87*, 542-554, doi:10.1111/bcp.14414.

55. Ge, S.; Mendley, S.R.; Gerhart, J.G.; Melloni, C.; Hornik, C.P.; Sullivan, J.E.; Atz, A.; Delmore, P.; Tremoulet, A.; Harper, B.; et al. Population Pharmacokinetics of Metoclopramide in Infants, Children, and Adolescents. *Clinical and Translational Science* **2020**, *13*, 1189-1198, doi:10.1111/cts.12803.

56. Maharaj, A.R.; Edginton, A.N. Physiologically Based Pharmacokinetic Modeling and Simulation in Pediatric Drug Development. *CPT: Pharmacometrics & Systems Pharmacology* **2014**, *3*, 1-13, doi:10.1038/psp.2014.45.

57. Miller, R.; Ewy, W.; Corrigan, B.W.; Ouellet, D.; Hermann, D.; Kowalski, K.G.; Lockwood, P.; Koup, J.R.; Donevan, S.; El-Kattan, A.; et al. How Modeling and Simulation Have Enhanced Decision Making in New Drug Development. *Journal of Pharmacokinetics and Pharmacodynamics* **2005**, *32*, 185-197, doi:10.1007/s10928-005-0074-7.